Quasistatic Resonators Based Triple-Mode Notched Microstrip Bandpass Filter

Shobha I. HUGAR [1], Jambunath S. BALIGAR [1], Veerendra DAKULAGI [2], K. M. VANITHA [3]

[1] Dept. of Electronics and Communication Engineering, Dr. Ambedkar Institute of Technology, Bengaluru, India
[2] Dept. of Electronics and Communication Engineering, Guru Nanak Dev Engineering College, Bidar, India
[3] Dept. of Electronics and Communication Engineering, M S Ramaiah Institute of Technology, Bengaluru, India

shobha_hugar@yahoo.co.in, jbaligar@gmail.com, veerendra.gndec@gmail.com, kmvanitha@msrit.edu

Submitted April 22, 2022 / Accepted November 23, 2022 / Online first January 30, 2023

Abstract. *This article discusses new approach for design and development of triple-mode notched microstrip bandpass filter based on quasistatic resonators (QR). The proposed approach is composed of two quasistatic resonant elements; Horizontal Plane Split Ring Resonator (HP-SRR), Vertical Plane Split Ring Resonator (VP-SRR) and a single Asymmetric Step Impedance Resonator (A-SIR) with parallel coupled feed structure. An additional attenuation pole realized by VP-SRR in desired passband tunes the dual-mode response to triple mode and enhances the 3dB bandwidth without changing the dimensions of basic the filter cell. The HP-SRR realizes a notch at WiMAX band (IEEE 802.11a lower band) in the desired passband. Further by changing the impedance of VP-SRR and HP-SRR both the location of additional attenuation pole frequency and notch band can be controlled. The proposed approach eliminates conventional method of realizing notch in the desired passband using vias and defective ground structures which have practical difficulties in realization and also the proposed approach results in compact notched wideband filter design.*

Keywords

Dual-mode, quasistatic resonators, asymmetric step impedance resonator, split ring resonators

1. Introduction

The continuous evolution in wireless communication technology demands advanced microwave components like compact filters. In literature a number of multimode bandpass filters such as dual-mode, triple-mode, quadruple-mode BPFs have been designed to meet the requirements of wireless communication industry. The dual-mode BPFs in [1–3] have been designed using closed loop, meandered dual-mode resonators like octagonal, hexagonal, star shaped resonators. The triangular, square patch resonators with corner cuts [4], [5] have also been proposed to design dual-mode BPFs. However all these reported filters have narrow bandwidth. Further to improve the bandwidth multimode resonators, coupled line structures and hairpin resonators have been proposed in [6–8]. But all these filters have larger footprint. The triple-mode BPFs reported in [9–11] have fabrication difficulties as they use via hole for grounding. Quadraple mode resonators have been used to design wideband filters in [12], [13]. Even through these filters provide wide bandwidth but have less frequency selective passband due to absence of transmission zeros at the passband edges. Besides these wideband BPFs, notched bandpass response filters have also been reported in literature since for some applications there is a need to avoid the interference from existing wireless communication systems such as WiMAX network. In literature these notched-band BPFs have been designed using parallel coupled T shaped SIR, trisection SIRs, parallel coupled trisection resonators with complementary split ring resonator (CSRR) [14–16], defective microstrip structures (DGS) [17–19]. Vias proposed in [20] to realize a notch are not practically feasible. Authors Jingbo Liu and Ting Zhang in [21], [22] have also proposed tuning of notch band frequency by varying length and width of via grooves and length of short stubs which has practical difficulties.

In this article, we propose a novel approach for design and development of triple-mode notched microstrip bandpass filter based on quasistatic resonators (QR); HP-SRR and VP-SRR. The proposed approach uses a single A-SIR with one step discontinuity as shown in Fig. 1. With proper selection of impedance ratio R and length ratio U for asymmetric stepped impedance resonator (A-SIR), first two resonant modes of the resonator are coupled to attain dual-mode response. Using parallel coupled feed structure, the two resonant modes of the resonator are coupled strongly and transmission zeros at upper and lower passband edges are realized to achieve high frequency selective passband. By integrating VP-SRR on low impedance sec-

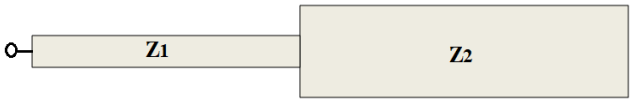

Fig. 1. Asymmetric step impedance resonator (A-SIR).

DOI: 10.13164/re.2023.0074

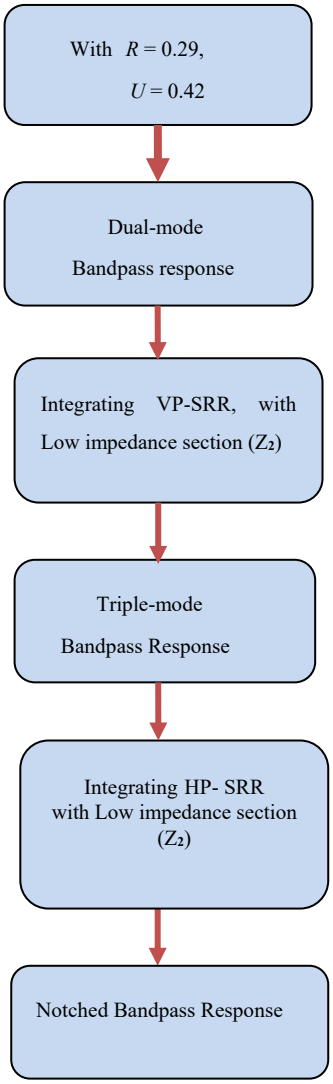

Fig. 2. Design flow for proposed approach.

tion of A-SIR, an additional attenuation pole is realized in desired passband at lower frequency side which has tuned the dual-mode response to triple-mode and also enhanced the 3dB bandwidth. Further triple-mode bandpass response is tuned to notched bandpass response by integrating HP-SRR on low impedance section of A-SIR. A notch-band is realized at 5.1 GHz (WiMAX band) within the 3dB passband to reject the radio frequency interference from WiMAX band. The proposed filter is designed and fabricated on RT/Duroid 5870 substrate having relative dielectric constant ε_r of 2.55, thickness h of 0.762 mm and loss tangent tan(δ) of 0.0009. Figure 2 depicts the design flow for proposed approach.

2. Analysis of Dual-Mode Response

As shown in Fig. 1 A-SIR consists of high and low impedance sections Z_1 and Z_2 with electrical lengths θ_1 and θ_2 respectively. The input impedance Z_{in} can be expressed as

$$Z_{in} = jZ_1 \frac{Z_1 - Z_2 \cot\theta_1 \cot\theta_2}{(Z_1 + Z_2)\cot\theta_2}. \quad (1)$$

Since at resonance, $Z_{in} = 0$, the above expression reduces to

$$1 - R\cot\theta_1 \cot\theta_2 = 0. \quad (2)$$

Here R is referred as impedance ratio and is calculated as the ratio of Z_2 to Z_1.The fundamental resonance frequency and higher order resonance frequencies of the resonator can be tuned over a wide range by varying R and electric length ratio U

$$U = \frac{\theta_2}{\theta_1 + \theta_2}. \quad (3)$$

By choosing appropriate values for R and U, the first two resonant modes of the resonator are coupled to realize dual-mode wideband response.

2.1 Dual-Mode Wideband BPF

A dual-mode wideband BPF shown in Fig. 3 is designed using A-SIR with one step discontinuity and parallel coupled feed structure. For an impedance ratio R of 0.29 [$Z_1 = 151\ \Omega$, $Z_2 = 39.75\ \Omega$] and electric length ratio U of 0.42 [$\theta_1 = 77°$, $\theta_2 = 56°$], the first two resonant modes of the resonator are coupled to attain dual-mode response. Parallel coupled feed structure contributes the transmission zeros at upper and lower passband edges [23] for good passband selectivity. Figure 4 depicts ADS simulation results of dual-mode wideband BPF.

It is seen from the simulation results shown in Fig. 4, that a wide passband exist from 1.6 GHz to 6.1 GHz with 3dB fractional bandwidth (FBW) of 82% centered at 3.1 GHz. The passband insertion loss S_{21} is 0.1 dB which is due to one step discontinuity [23] and in-band return loss S_{11} is greater than 10 dB. The S_{11} curve validates the dual-mode operation with two pole frequencies located at 3.12 GHz and at 4.65 GHz. The transmission zeros at 1.6 GHz (lower passband edge) with attenuation level of more than 70 dB and at 6.1 GHz (upper passband edge) with attenuation level of 70 dB are by the virtue of parallel coupled feed and indicates a high frequency selective passband. It can also be noted that the upper and lower rejection bands are at rejection levels of 28 dB and 30 dB respectively. The additional two transmission zeros are also

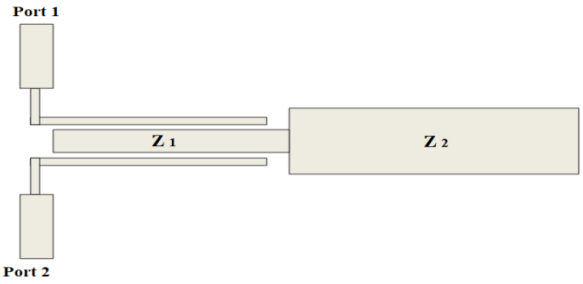

Fig. 3. Dual-mode wideband BPF.

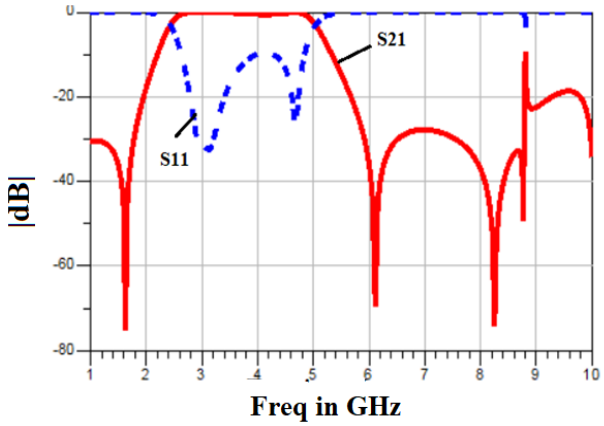

Fig. 4. Dual-mode wideband response.

reported in the upper rejection band at 8.2 GHz and at 8.8 GHz with attenuation level of 75 dB and 45 dB respectively.

3. Analysis of Triple-Mode Response

A microstrip quasistatic resonator element, split ring resonator (SRR) shown in Fig. 5(a) is used to realize triple-mode response and it behaves as LC resonator circuit [24]. The lumped model for the resonator is as shown in Figs. 5(b) and (c).

In Fig. 5(b) and (c), C is total capacitance between the rings and C_s is the series capacitance of the upper and lower halves of the resonator. The resonance frequency of quasistatic resonator is $f_r = 1/[2\pi(LC)^{1/2}]$. The inductance L can be approximated by that of a single ring with averaged radius and width [24].The deployment of this resonating element on low impedance section (Z_2) of A-SIR in vertical plane as shown in the inset of Fig. 6(a) results in realization of additional attenuation pole (Pole3) in the desired passband. The simulated triple-mode response is shown in Fig. 6(a). It is interesting to mention here that the additional attenuation pole frequency is reported at resonance frequency of VP-SRR. With series capacitance $C_s = 10$ pF and inductance $L = 0.32$ nH, the additional attenuation pole frequency is realized at 2.8 GHz. With triple-mode response the 3dB FBW achieved is 95.6% which is comparatively more than dual-mode response. The in-band return loss S_{11} is greater than 10 dB and insertion loss is 0.1 dB in the entire passband. Further the location of additional attenuation pole frequency can be controlled by changing the impedance Z of VP-SRR as shown in Fig. 6(b).

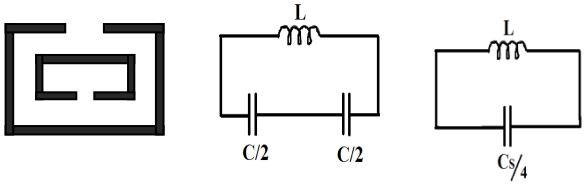

(a) (b) (c)

Fig. 5. (a) Split ring resonator (SRR). (b) Lumped model. (c) Equivalent lumped model.

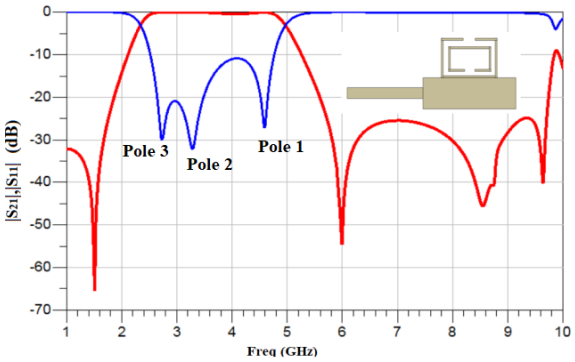

(a)

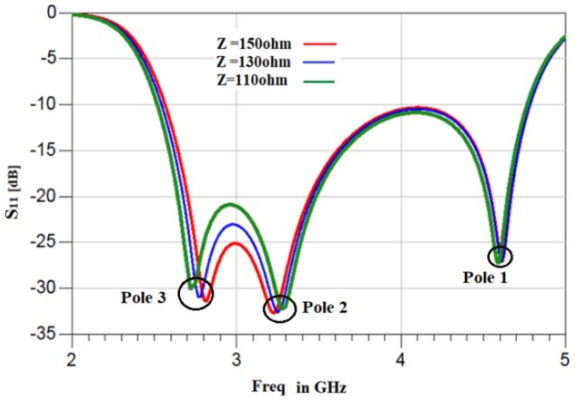

(b)

Fig. 6. (a) Triple mode response. (b) Shift in location of additional pole frequency.

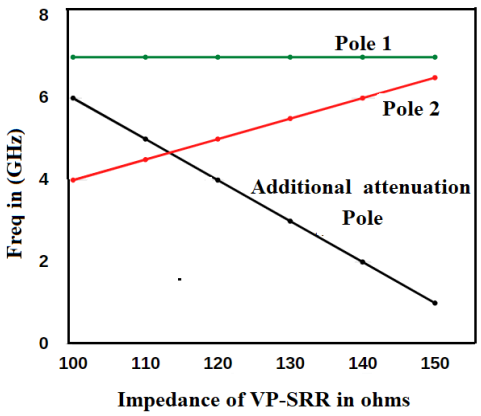

Fig. 7. Pole frequencies vs. impedance of VP-SRR.

Here the impedance Z of VP-SRR is varied in range of 110 Ω–150 Ω and corresponding shift in the location of Pole3 frequency is shown in Fig. 7. The varying impedance Z of VP-SRR also varies slightly the location of Pole2.

4. Design and Analysis of Notch-Band Response

In this work we have proposed a new approach to realize a notched bandpass response with compact filter configuration. Further the notch-band is realized at 5.1 GHz (WiMAX band - IEEE 802.11a lower band). In the

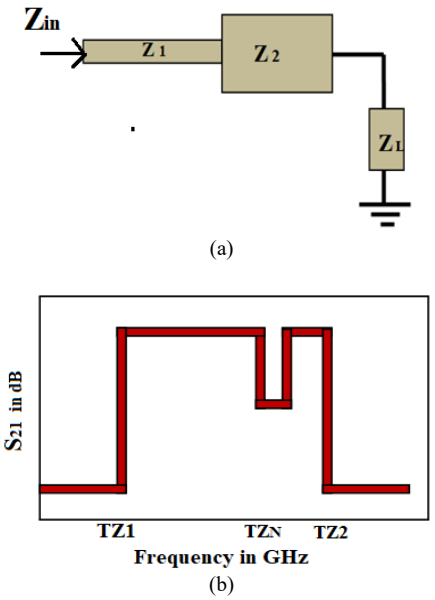

Fig. 8. (a) A-SIR terminated with Z_L. (b) Conceptual response.

proposed approach, the low impedance section Z_2 is terminated with a reactive impedance Z_L as shown in Fig. 8(a) which realizes a new transmission zero TZ_N along with two inherent transmission zeros TZ_1 and TZ_2 of the A-SIR. The conceptual response for the proposed configuration is shown in Fig. 8(b). The new transmission zero TZ_N is due to the reactive impedance Z_L and it realizes a notch band in desired passband.

For instance in this work, the existence of three transmission zeros TZ_1, TZ_2 and TZ_N in the proposed configuration is shown mathematically. To validate the three transmission zeros, the input impedance Z_{in} for the proposed configuration is given

$$Z_{in} = jZ_2 \frac{R_1 + \tan\theta_2 \tan\theta_L + \dfrac{\tan\theta_1}{R_2}\left(\tan\theta_L + R_1 \tan\theta_2\right)}{\tan\theta_L + R_1 \tan\theta_2 R_1 R_2 \tan\theta_2 - R_2 \tan\theta_1 \tan\theta_2 \tan\theta_L}. \tag{4}$$

Here the impedance ratios R_1, R_2 are $R_1 = Z_L/Z_2$ and $R_2 = Z_2/Z_1$. With $\theta_1 = \theta_2 = \theta_3 = \theta_4$ the numerator of (4) is equated to null and is simplified as function F in terms of R_1, R_2 and the electrical length θ as given by (5)

$$F = -R_1 + \tan^2\theta + \frac{\tan^2\theta}{R_2}\left(1 + R_1\right). \tag{5}$$

According to our design considerations, with $R_1 = 3.9$ and $R_2 = 0.3$, the function F can be graphically plotted in terms of electrical length θ as shown in Fig. 9.

Figure 9 depicts existence of three transmission zeros TZ_1, TZ_2 and TZ_N with the proposed approach and the new transmission zero (TZ_N) realizes a notch in desired passband. In this work the reactive impedance Z_L is realized by a split ring resonator and is connected with low impedance section Z_2 in horizontal plane (HP-SRR) as shown in Fig. 10(a). A notch-band is realized at fundamental resonance frequency of HP-SRR. In Fig. 10(b) the simulated response of the proposed filter configuration is shown. The optimized dimensions of the proposed filter are: $L_1 = 10.2$ mm, $L_2 = 15$ mm, $L_3 = 13.5$ mm, $L_4 = 1.6$ mm, $L_5 = 1.5$ mm, $L_6 = L_7 = 2.8$ mm, $L_8 = 2.8$ mm, $L_9 = 4.4$ mm, $L_{10} = 1.2$ mm, $L_{11} = 3.8$ mm, $L_{12} = 1.9$ mm, $L_{13} = 0.6$ mm, $W_1 = 3.2$ mm, $W_2 = 0.3$ mm, $W_3 = 0.2$ mm, $W_4 = 1$ mm and the distance between two rings is 0.2 mm.

The simulation results shown in Fig. 10(b) report a wide passband from 1.45 GHz to 6.33 GHz with 3dB FBW of 111% centered at 3.1 GHz. The insertion loss S_{21}

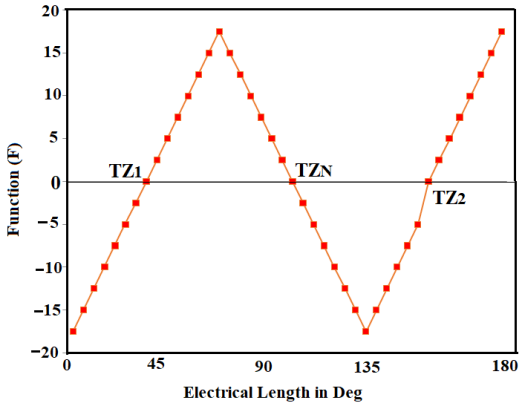

Fig. 9. Function F versus electrical length θ.

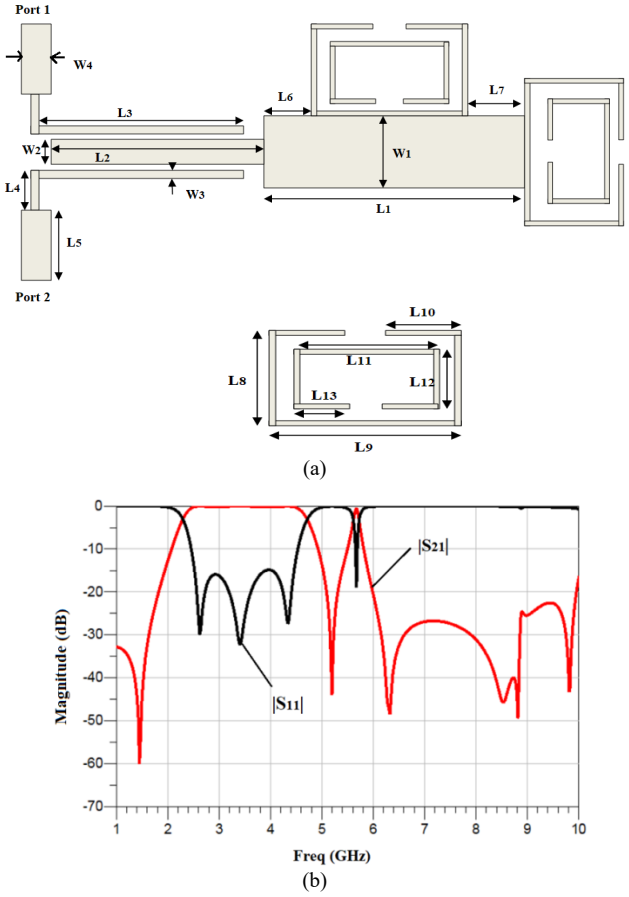

Fig. 10. (a) Proposed notched wideband BPF. (b) Simulated notched bandpass response.

Response	FBW in %
Dual-mode(without VP/HP SRR)	82
Triple mode(With VP-SRR)	95.6
Triple mode notched(With VP and HP SRR)	111

Tab. 1. FBW reported in different responses.

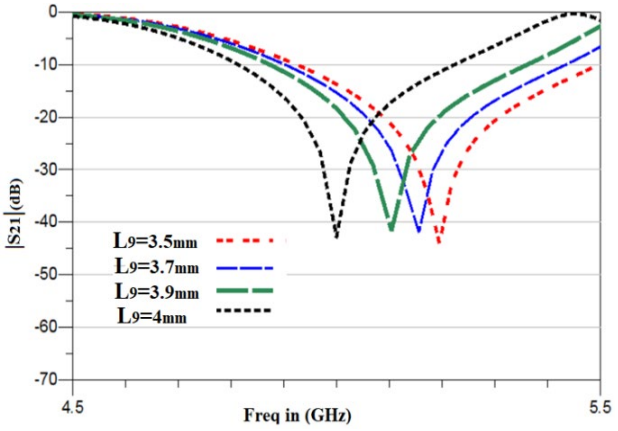

Fig. 11. Tuning of notch band.

in entier passband is 0.1 dB and return loss S_{11} is better than 10 dB in the passband. A notch band is reported at 5.1 GHz with attenuation level of 45 dB and 3dB bandwidth of 100 MHz. The transmission zeros in upper rejection band at 8.22 GHz and at 9.8 GHz with attenuation level of 50 dB and 45 dB respectively ensure 3470 MHz upper rejection bandwidth. Table 1 summerizes percentage of FBW achieved in dual-mode, triple-mode and notched bandpass responses.

5. Controlled Notchband

Further it is important to note here that the location of notch-band can be cotrolled by varying the side length L_9 of HP-SRR as shown in Fig. 11. Here the notch frequency is controlled in range of 5 GHz–5.2 GHz by varying L_9 from 4 mm to 3.5 mm in simulation. It is interesting to mention here that with changing L_9 the inband standing waves remain stationary which manifests good impedance matching between the resonator and the input ports.

6. Experimental Results

For experimental validation, the two proposed filter configurations shown in Figs. 6(a) and 10(a) are fabricated on RT/Duroid 5870 substrate with thickness h of 0.762 mm, loss tangent(δ) of 0.0009 and relative dielectric constant ε_r of 2.55. The photographs of fabricated filters Filter A and Filter B are shown in Figs. 12(a) and (b). The measured frequency responses are obtained by means of the Agilent 8719ES vector network analyzer with measuring frequency range from 50 MHz to 13.5 GHz. Both measured and simulated frequency responses for Filter A and Filter B are shown in Figs. 13(a)–(d). Good agreement between measured and simulated responses is seen, except for the frequency shift, which is mainly caused by fabrica-

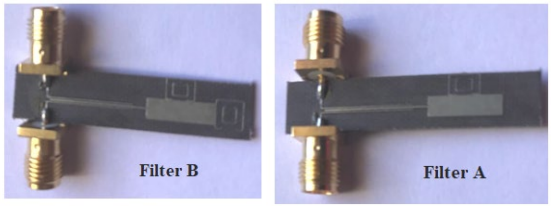

(a) (b)

Fig. 12. Photographs of fabricated filters: (a) Filter A - Triple mode BPF. (b) Filter B - Notched wideband BPF.

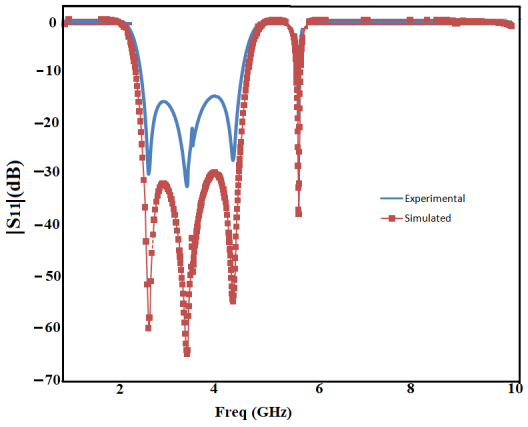

(a)

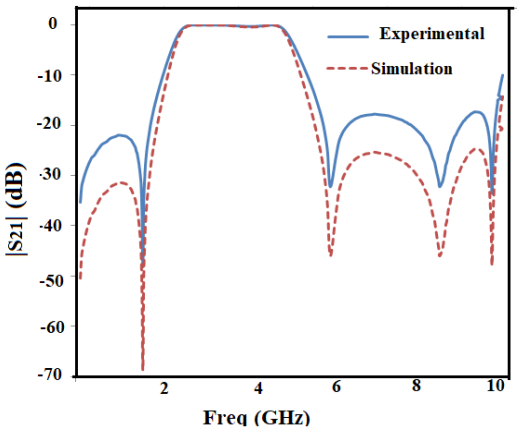

(b)

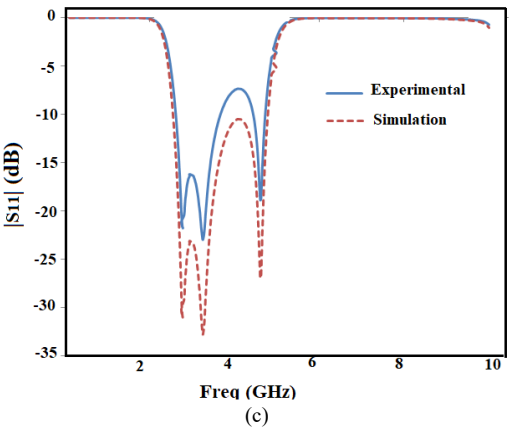

(c)

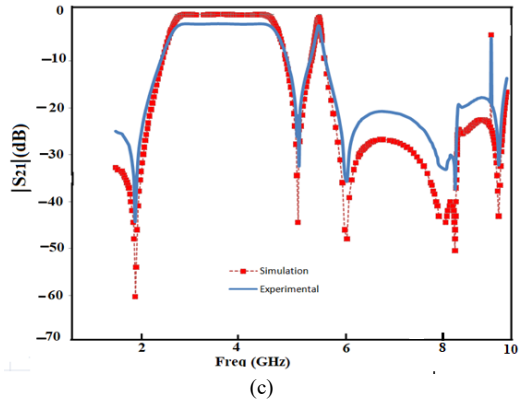

Fig. 13. (a), (b) Measured and simulated responses for Filter A. (c), (d) Measured and simulated responses for Filter B.

tion tolerance and variation in physical characteristic such as relative dielectric constant ε_r. RT/Duroid 5870 has ±2% dielectric tolerance which impacts the effective dielectric constant ε_{eff} and hence the guided wavelength λ_g [25]. In this design ±2% tolerance results in $2.154 \leq \varepsilon_{eff} \leq 2.184$ and hence the 23 mm $\leq \lambda_g \leq$ 27 mm. Due to these variations the minimum and maximum shift in measured frequency expected is 100 MHz and 300 MHz.

The measured fractional bandwidth with triple-mode response is 92.3% at measured center frequency of 2.9 GHz. The measured insertion loss S_{21} in passband is 1.2 dB which is more than the simulated one and is due to circuit losses; conductor losses, dielectric losses and radiation loss and is also due to SMA (Sub-Miniature A Type) connectors losses. With notched response, the measured FBW is 109% at measured center frequency of 2.9 GHz. The notch band is located at 4.85 GHz in experimental results. The lower attenuation levels for transmission zeros in experimental results may be due to the surface resistivity of the dielectric substrate. In Tab. 2 the presented filter performance is compared with the filters reported in literature.

7. Conclusion

A new approach for design and development of triple-mode notched microstrip bandpass filter based on quasistatic resonators (QR) is discussed in this article. The dual-mode property of the A-SIR has been investigated. A new applications of split ring resonators in design of triple mode notched BPF have been presented for the first time in this article. The resonance charecteristics of SRR are investigated based on its lumped circuit model to obtain insight regarding position of SRRs for triple mode notched bandpass response. It is found that by connecting SRRs in vertical (VP-SRR) and horizontal planes (HP-SRR), triple mode response with increased bandwidth and notched bandpass responses can be achieved respectively. By varying the impedances of VP-SRR and HP-SRR elements, the locations of additional attenuation pole frequency and notch band can be tuned respectively. The designed filter not only has good skirt factor and FBW but also has a compact size of 30.34 mm × 8.1 mm. The proposed filter configuration is useful for Cognitive Radios systems since location of poles and notch-band can be controlled.

References

[1] ESFEH, B. K., ISMAIL, A., ABDULLAH, R. S. A. R., et al. Compact narrowband bandpass filter using dual-mode octagonal meandered loop resonator for Wimax application. *Progress In Electromagnetics Research B*, 2009, vol. 16, p. 277–290. DOI: 10.2528/PIERB09061601

[2] LA, D. S., JIA, S. Q., MA, X. L. Compact wideband band-pass filter using regular hexagon ring resonator. In *Proceedings of the IEEE Asia-Pacific Microwave Conference (APMC)*. Nanjing (China), 2015, vol. 1, p. 1–3. DOI: 10.1109/APMC.2015.7411709

[3] AVINASH, K. G., SRINIVASA RAO, I. Design of bandpass filter using star loop dual mode resonator. In *Proceedings of the IEEE International Conference on Communications and Signal Processing (ICCSP)*. Melmaruvathur (India), 2015, p. 0238–0241. DOI: 10.1109/ICCSP.2015.7322877

Parameter / Ref	[21] 2019	[26] 2018	[27] 2017	[28] 2019	[29] Exp 2 2020	**This work**
Center frequency (GHz)	5	3	2.3	4/8	4.1/8	**3.1**
S_{11} (dB)	12	11.7	>13	10	10	**>10**
S_{21} (dB)	1.2	2.1	0.35	NA	1.2/2.8	**0.1**
FBW (%)	100	107	80	108	101	**111**
No of notches	1	1	2	1	1	**1**
Tunable notch	**No**	**No**	**No**	**No**	**No**	**Yes**

Tab. 2. Performance comparison.

[4] AVINASH, K. G., SRINIVASA RAO, I. Highly selective dual-mode microstrip bandpass filters using triangular patch resonators. *Advanced Electromagnetics,* 2017, vol. 6, no. 1, p. 77–84. DOI: 10.7716/aem.v6i1.469

[5] MEZAAL, Y. S., EYYUBOGLU, H. T. Investigation of new microstrip bandpass filter based on patch resonator with geometrical fractal slot. *PLOS One*, 2016, vol. 11, no. 4, p. 1–12. DOI: 10.1371/journal.pone.0152615

[6] LEE, K. C., SU, H. T., HALDAR, M. K. A modified hair-pin resonator for the design of compact bandpass filter with suppression of even harmonics. *Progress In Electromagnetics Research C,* 2012, vol. 31, p. 241–253. DOI: 10.2528/PIERC12050808

[7] HUGAR S. I., MUNGURWADI, V., BALIGAR, J. S. Novel approach for center frequency and bandwidth tuning in multimode resonator based microstrip dual-mode bandpass filter. *Procedia Computer Science*, 2020, vol. 171, p. 2067–2072. DOI: 10.1016/j.procs.2020.04.222

[8] ZHANG, B., WU, Y., LIU, Y. Wideband single-ended and differential bandpass filters based on terminated coupled line structures. *IEEE Transactions on Microwave Theory and Techniques,* 2016, vol. 65, no. 3, p. 761–774. DOI: 10.1109/TMTT.2016.2628741

[9] LEE, K. C., SU, H. T., HALDAR, M. K. A novel compact triple-mode resonator for microstrip bandpass filter design. In *Proceeding of Asia Pacific Microwave Conference.* Yokohama (Japan), 2010, p. 1871–1874. ISBN: 978-4-902339-22-2

[10] CHEN, C.-F., SHEN, T.-M., HUANG, T. Y., et al. Design of compact microstrip quadruplexer based on the tri-mode net-type resonators. *IEEE Microwave and Wireless Component Letters*, 2011, vol. 21, no. 10, p. 534–536. DOI: 10.1109/LMWC.2011.2165278

[11] SOVUTHY, C., WEN, W. P. Microwave planar triple-mode resonator filter. In *the Proceeding of National Postgraduate Conference (NPC)*. Perak (Malaysia), 2011, p. 1–3. DOI: 10.1109/NatPC.2011.6136425

[12] LEE, K. C., SU, H. T., HALDAR, M. K. Compact quadruple-mode resonator for wideband bandpass filter design. *IET Microwaves, Antennas & Propagation*, 2014, vol. 8, no. 3, p. 67–72. DOI: 10.1049/iet-map.2013.0021

[13] DENG, H.-W., ZHAO, Y.-J., ZHANG, L., et al. Quadruple-mode stub-loaded resonator and broadband BPF. *Progress In Electromagnetics Research Letters*, 2010, vol. 18, p. 1–8. DOI: 10.2528/PIERL10061713

[14] NOSRATI, M., DANESHMAND, M. Compact microstrip ultra-wideband double/single notch-band band-pass filter based on wave's cancellation theory. *IET Microwaves, Antennas & Propagation,* 2012, vol. 6, no. 8, p. 862–868. DOI: 10.1049/iet-map.2011.0519

[15] BORAZJANI, O., NOSRATI, M., DANESHMAND, M. A novel triple notch-bands ultra wide-band band-pass filters using parallel multi-mode resonators and CSRRs. *International Journal of RF and Microwave Computer-Aided Engineering*, 2013, vol. 24, no. 3, p. 375–381. DOI: 10.1002/mmce.20770

[16] NOSRATI, M., DANESHMAND, M. Developing single-layer ultra-wideband band-pass filter with multiple (triple and quadruple) notches. *IET Microwaves Antennas & Propagation*, 2013, vol. 7, no. 8, p. 612–620. DOI: 10.1049/iet-map.2013.0022

[17] ZHENG, X., PAN, Y., JIANG, T. UWB bandpass filter with dual notched bands using T-shaped resonator and L-shaped defected microstrip structure. *Micromachines*, 2018, vol. 9, no. 6, p. 280–291. DOI: 10.3390/mi9060280

[18] AZIZI, S., EL GHARBI, M., AHYOUD, S., et al. Design and analysis of compact microstrip UWB band pass filter with a notched band using defected microstrip structure. *Procedia Manufacturing*, 2019, vol. 32, p. 669–674. DOI: 10.1016/j.promfg.2019.02.269

[19] SHAMAN, H. N., ALMORQI, S. K., ALAMOUDI, A. O. High-selectivity microstrip bandpass filter with notch-band for wideband wireless applications. In *Proceedings of IEEE International Conference on Microwaves, Radar and Wireless Communications*. Gdansk (Poland), 2014, p. 1–4. DOI: 10.1109/MIKON.2014.6899938

[20] LI, Q., LIANG, C.-H., WEN, H.-B., et al. Compact planar ultra-wideband (UWB) bandpass filter with notched band. In *Proceedings of IEEE Asia Pacific Microwave Conference*. Singapore, 2009, p. 1–4. DOI: 10.1109/APMC.2009.5385380

[21] LIU, J., DING, W., CHEN, J., et al. New ultra-wideband filter with sharp notched band using defected ground structure. *Progress In Electromagnetics Research Letters*, 2019, vol. 83, p. 99–105. DOI: 10.2528/PIERL18111302

[22] ZHANG, T., BAO, J., CAI, Z., et al. A C-band compact wideband bandpass filter with high selectivity and improved return loss. *IEEE Microwave and Wireless Components Letters,* 2018, vol. 28, no. 9, p. 824–829. DOI: 10.1109/LMWC.2018.2860245

[23] CHANG, Y.-C., KAO, C.-H., WENG, M.-H. A compact wideband bandpass filter using single asymmetric SIR with low loss and high selectivity. *Microwave and Optical Technology Letters*, 2008, vol. 51, no. 1, p. 242–244. DOI: 10.1002/mop.24023

[24] BAENA, J. D., BONACHE, J., MARTIN, F., et al. Equivalent-circuit models for split-ring resonators and complementary split-ring resonators coupled to planar transmission lines. *IEEE Transactions on Microwave Theory and Techniques*, 2005, vol. 53, no. 4, p. 1451–1461. DOI: 10.1109/TMTT.2005.845211

[25] MABROUK, M., BOUSBIA, L. Study and enhanced design of RF dual band bandpass filter validation and confirmation of experimental measurements. *Circuits and Systems*, 2011, vol. 2, no. 4, p. 293–296. DOI: 10.4236/cs.2011.24041

[26] JI, X. C., JI, W. S., FENG, L. Y., et al. Design of a novel multi-layer wideband bandpass filter with a notched band. *Progress In Electromagnetics Research Letters*, 2019, vol. 82, p. 9–16. DOI: 10.2528/PIERL18121101

[27] YANG, L., CHOI, W. W., TAM, K. W., et al. Novel wideband bandpass filter with dual notched bands using stub-loaded resonators. *IEEE Microwave and Wireless Component Letters*, 2017, vol. 27, no. 1, p. 25–27. DOI: 10.1109/LMWC.2016.2629967

[28] WENG, M. H., HSU, C. W., LAN, S. W., et al. An ultra-wideband bandpass filter with a notch band and a wide upper bandstop performances. *Electronics*, 2019, vol. 8, no. 11, p. 1–10. DOI: 10.3390/electronics8111316

[29] ZHANG, P., LIU, L., CHEN, D., et al. Application of a stub-loaded square ring resonator for wideband bandpass filter design. *Electronics*, 2020, vol. 9, no. 1, p. 1–14. DOI: 10.3390/electronics9010176

About the Authors …

Shobha HUGAR is currently working as an Assistant Professor in the Department of Electronics and Communication Engineering at Sapthagiri College of Engineering, Bangalore, India. She received her Ph.D. degree in RF and Microwave Passive Filters from Visvevsaraya Technological University, Belagavi, India in 2022. She received the B.E. and M.Tech. degrees in Electronics and Communication Engineering and VLSI Design and Embedded Systems

from Karnataka University, Dharwad, Visvevsaraya Technological University, Belagavi, India, in 2000 and 2008, respectively. Her research interest are RF & microwaves, antenna and CMOS RF circuit design.

Jambunath S. BALIGAR is currently working as an Associate Professor in the Department of Electronics and Communication Engineering at Dr. Ambedkar Institute of Technology, Bangalore, India. He received his Ph.D. degree from Bangalore University, India, in 2000. He is working in the area of RF and microwave antenna. He has published papers in IEEE Electronics Letters and Microwave and Optical Technology Letters.

Veerendra DAKULAGI earned his B.E. in Electronics and Communication Engineering and his M.Tech. in Power Electronics from the Visvesvaraya Technological University, Belagavi, India, in 2007 and 2011, respectively. He received his Ph.D. degree in Array Signal Processing from the same university in 2018. He was a Post Doctoral Fellow of Electrical Engineering Dept., LUC Malaysia in 2019–2021. From May 2022 to December 2022, he is INSA visiting scientist to IIT Delhi. Currently, he is working as an Associate Professor in Electronics and Communication Engineering Department, Guru Nanak Dev Engineering College, Bidar, Karnataka, India. His research interests are in signal processing and communications, including statistical and array signal processing, adaptive beamforming, spatial diversity in wireless communications, and multiuser and MIMO communications.

VANITHA K. M. is currently working as an Assistant Professor in the Department of Electronics & Instrumentation Engineering at M. S. Ramaiah Institute of Technology. Bangalore, India. She received the B.E. and M.Tech. degrees in Electronics and Communication Engineering and VLSI Design and Embedded Systems from Bengaluru University, Visvevsaraya Technological University, Belagavi, India, in 2000 and 2008, respectively.